Electronic Supplementary Information – First-principles study of interfacial vacancies in β-$CsPbI_3$/1T-MoS_2 heterostructure towards photocatalytic applications

Chol-Hyok Ri[a,c], Se-Hun Pak[a], Song-Il O[a], Chol-Su Jang[a], Yu-Song Kim[b], Jin-Song Kim[c] and Chol-Jun Yu[c*]

[a] *Faculty of Physics, O Jung Hup Chongjin University of Education, Chongjin, North Hamgyong Province, Democratic People's Republic of Korea*

[b] *Mathematics Department, Chongjin University of Mining and Metallurgical Engineering, Chongjin, North Hamgyong Province, Democratic People's Republic of Korea*

[c] *Chair of Computational Materials Design, Faculty of Materials Science, **Kim Il Sung** University, Ryongnam-Dong, Taesong District, Pyongyang, PO Box 76, Democratic People's Republic of Korea*

Table S1. The lattice constants of β-$CsPbI_3$ and 1T-MoS_2 calculated with various exchange-correlation functionals (unit: Å).

Systems	Space group	This work				Previous work	
		PBE	PBEsol	PBE+XDM	vdW-DF-ob86	DFT cal.	Exp.
β-$CsPbI_3$	$P4/mbm$	8.806, 6.463	8.599, 6.343	8.492, 6.325	8.625, 6.390	8.447, 6.273[a]	8.826, 6.290[b]
1T-MoS_2	$P\bar{3}m1$	3.208, 6.929	3.227, 5.875	3.203, 5.836	3.190, 5.711	3.18[c] 3.19[d]	3.23, 5.99[e]

[a] Calculated with HSE06 functional [1]
[b] Ref. [2]
[c] Calculated with GGA-PBE functional [3]
[d] Calculated with HSE06 functional [4]
[e] Ref. [5]

*Corresponding author: Chol-Jun Yu, Email: cj.yu@ryongnamsan.edu.kp

Table S2. Total energies calculated for CsI/MoS_2 and PbI_2/MoS_2 heterostructures with all possible interfacial vacancies.

	Cs vacancy		Pb vacancy		I vacancy		S vacancy	
Interface Systems	Number	Energy (eV)	Number	Energy (eV)	Number	Energy (eV)	Number	Energy (eV)
CsI/MoS_2	1	−23810.8608	–	–	1	−23590.5371	1	−23625.2869
	2	**−23810.8784**	–	–	2	−23590.5063	2	−23625.5660
	3	−23810.8543	–	–	**3**	**−23590.5738**	3	−23625.1397
	4	−23810.8165	–	–	4	−23590.5136	4	−23625.5653
							5	−23625.6172
							6	−23624.9196
							7	−23625.4481
							8	−23624.9829
							9	−23625.2995
							10	**−23625.6983**
							11	−23625.4272
							12	−23625.0811
							13	−23625.3628
							14	−23625.6806
							15	−23625.5701
							16	−23625.3124
							17	−23625.6792
PbI_2/MoS_2	–	–	1	−25085.9734	1	−24872.5075	1	−24907.0809
	–	–	2	−25085.8119	2	−24872.4364	2	−24907.4264
	–	–	**3**	**−25086.4856**	**3**	**−24873.1253**	3	−24906.7423
	–	–	4	−25085.9657	4	−24872.3062	4	−24906.6897
					5	−24872.4825	5	−24907.4099
					6	−24872.5717	6	−24906.4367
					7	−24872.6004	7	−24907.1396
					8	−24872.5717	8	−24907.5173
							9	−24907.3191
							10	−24906.6443
							11	−24907.7578
							12	−24908.5292
							13	−24907.0801
							14	−24907.1407
							15	**−24907.9077**
							16	−24906.9137
							17	−24908.2532

Table S3. The Fermi level E_F^s, valence band maximum level E_{VB}, conduction band minimum level E_{CB}, electrostatic potential bottom at the middle layer V_{bot} and Fermi energy correction ΔV_F for MoS_2 and $CsPbI_3$ surfaces with CsI and PbI_2 terminations (unit: eV).

Surface	E_F^s	E_{VB}	E_{CB}	V_{bot}	ΔV_F
MoS_2	−3.94			−13.36	−9.42
CsI	−2.75	−3.55	−1.98	−3.79	−1.04
PbI_2	−2.75	−3.55	−1.98	−9.15	−6.40

Table S4. The calculated Fermi level of interface E_F, vacuum level ϕ_{vac}, and electrostatic potential bottom at the middle layer V_{bot} and Fermi level E_F^i for MoS_2 and $CsPbI_3$ sides in the interface systems (unit: eV).

Interface		E_F	ϕ_{vac}	V_{bot,MoS_2}	$V_{bot,CsPbI_3}$	E^i_{F,MoS_2}	$E^i_{F,CsPbI_3}$
CsI/MoS_2	pristine	–4.01	0.47	–12.16	–3.66	–2.74	–2.62
	V_{Cs}	–4.05	0.45	–12.11	–3.61	–2.69	–2.57
	V_I	–3.69	0.74	–11.84	–3.94	–2.42	–2.90
	V_S	–4.02	0.74	–12.12	–3.66	–2.70	–2.62
PbI_2/MoS_2	pristine	–3.50	0.87	–11.85	–8.64	–2.43	–2.24
	V_{Pb}	–4.64	0.01	–12.71	–8.04	–3.29	–1.64
	V_I	–4.44	0.15	–12.50	–8.37	–3.08	–1.97
	V_S	–4.49	0.04	–12.65	–8.38	–3.23	–1.98

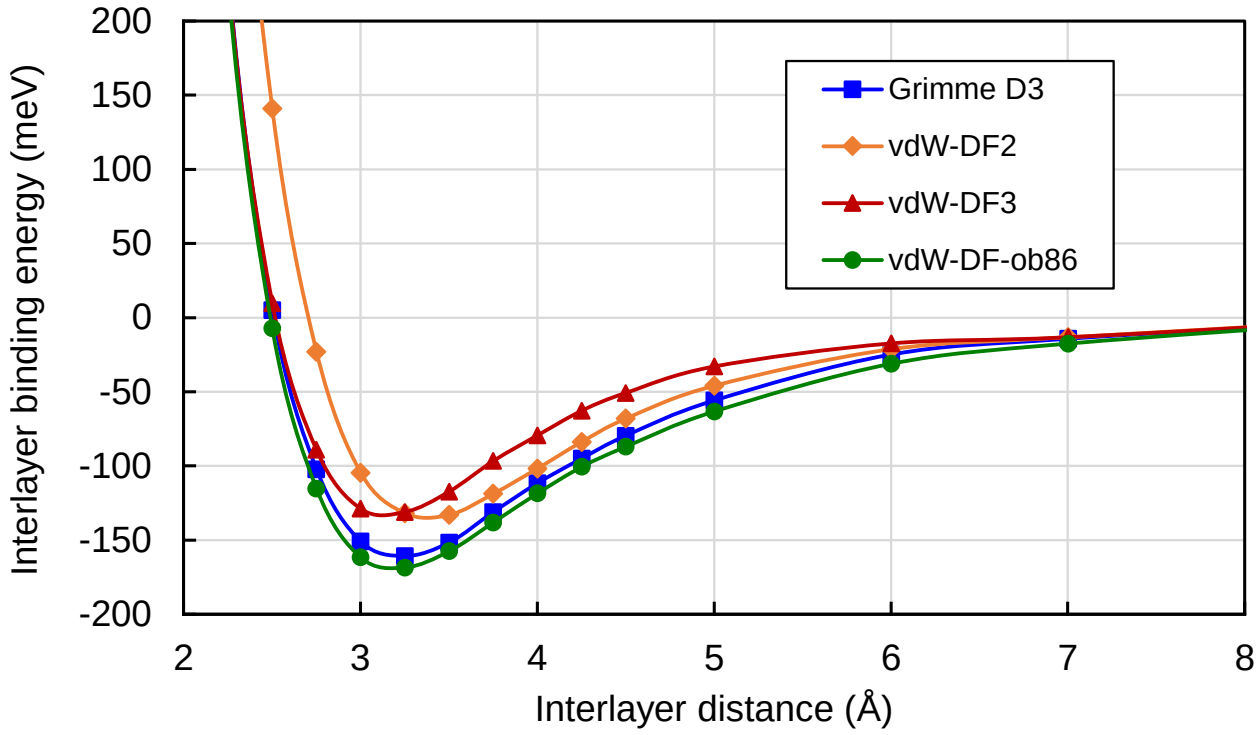

Fig. S1 Interlayer binding energy per atom as a function of interlayer distance for pristine PbI_2/MoS_2 interface, calculated using different XC functionals with different dispersion corrections, including the Grimmes's D3, vdW-DF2 and vdW-DF3.

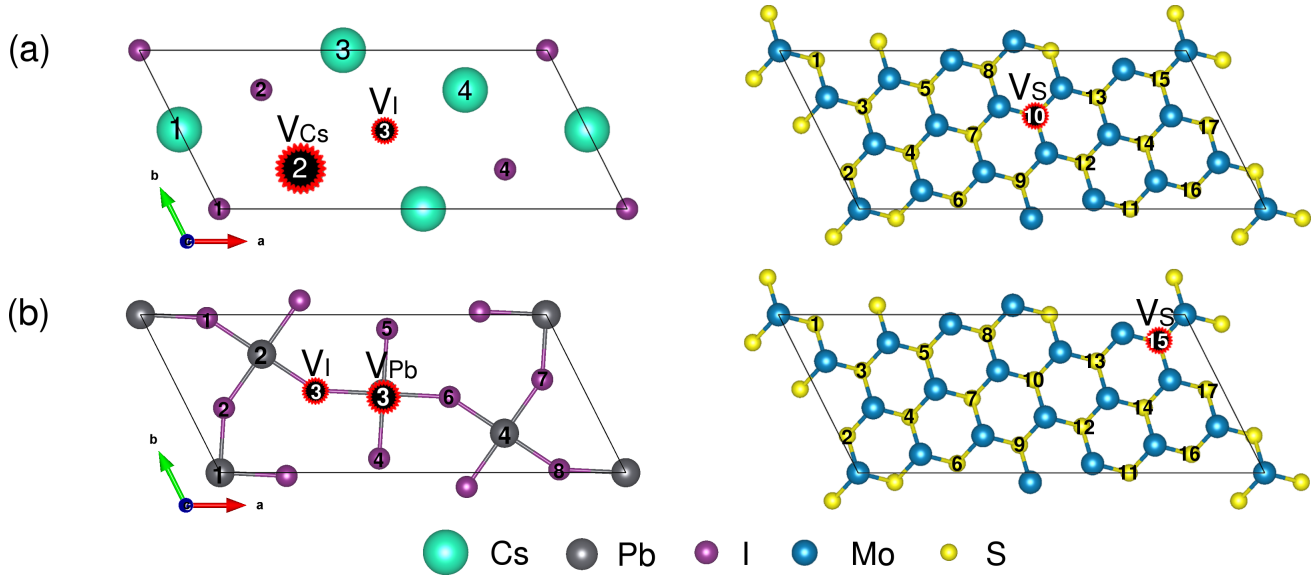

Fig. S2 All vacancy sites included in the calculation for CsI/MoS_2 (a) and PbI_2/MoS_2 (b) heterostructures. The circles filled with black with red borders represent vacancy sites with the minimum energy.

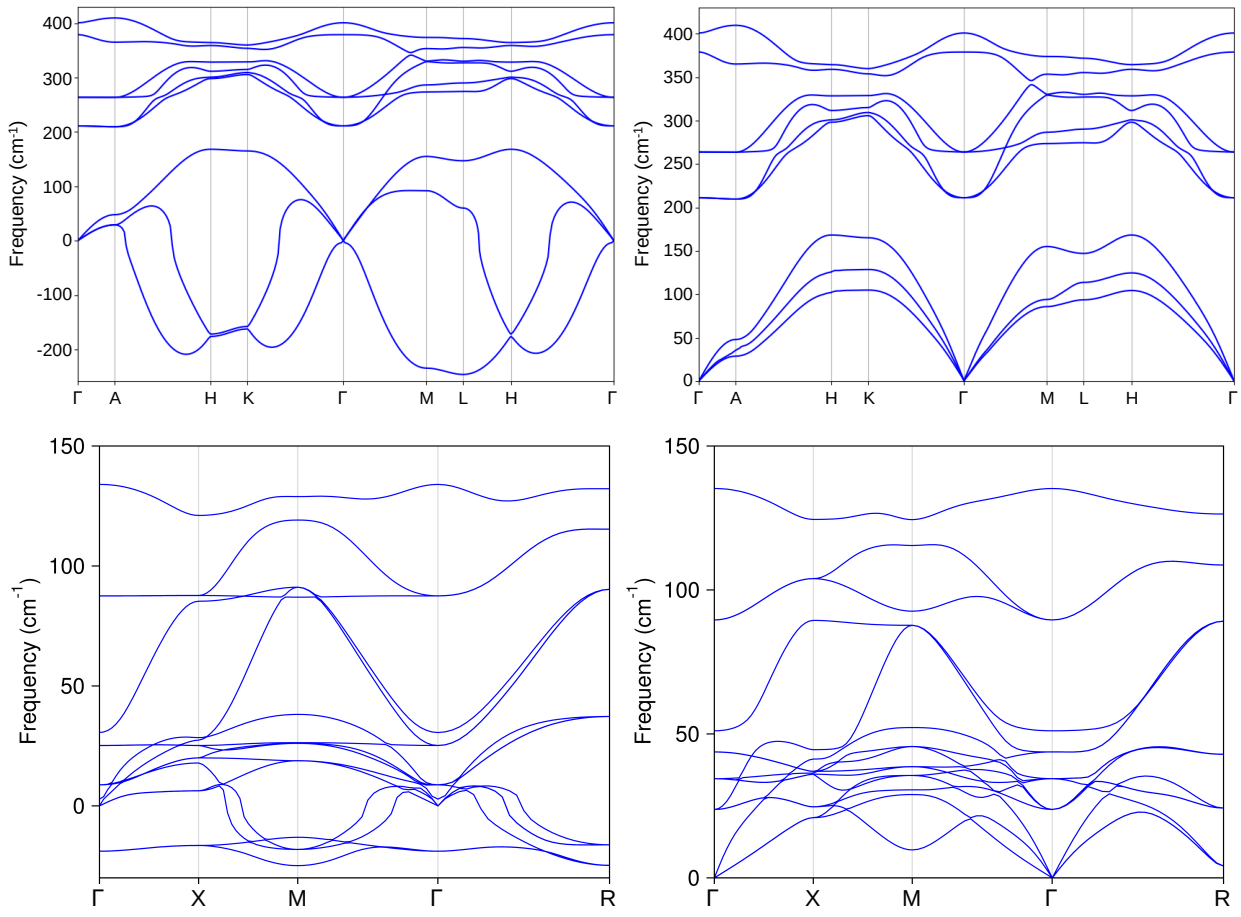

Fig. S3 Phonon dispersion curves of bulk 1T-MoS_2 (top panel) and β-$CsPbI_3$ (bottom panel). For both bulks, the phonon dispersion curves calculated at 0 K (left panel) contain the soft-mode with imaginary frequency, but those calculated at room temperature using the self-consistent phonon approach [6] (right panel) do not contain any soft-modes, indicating their thermodynamic stabilities.

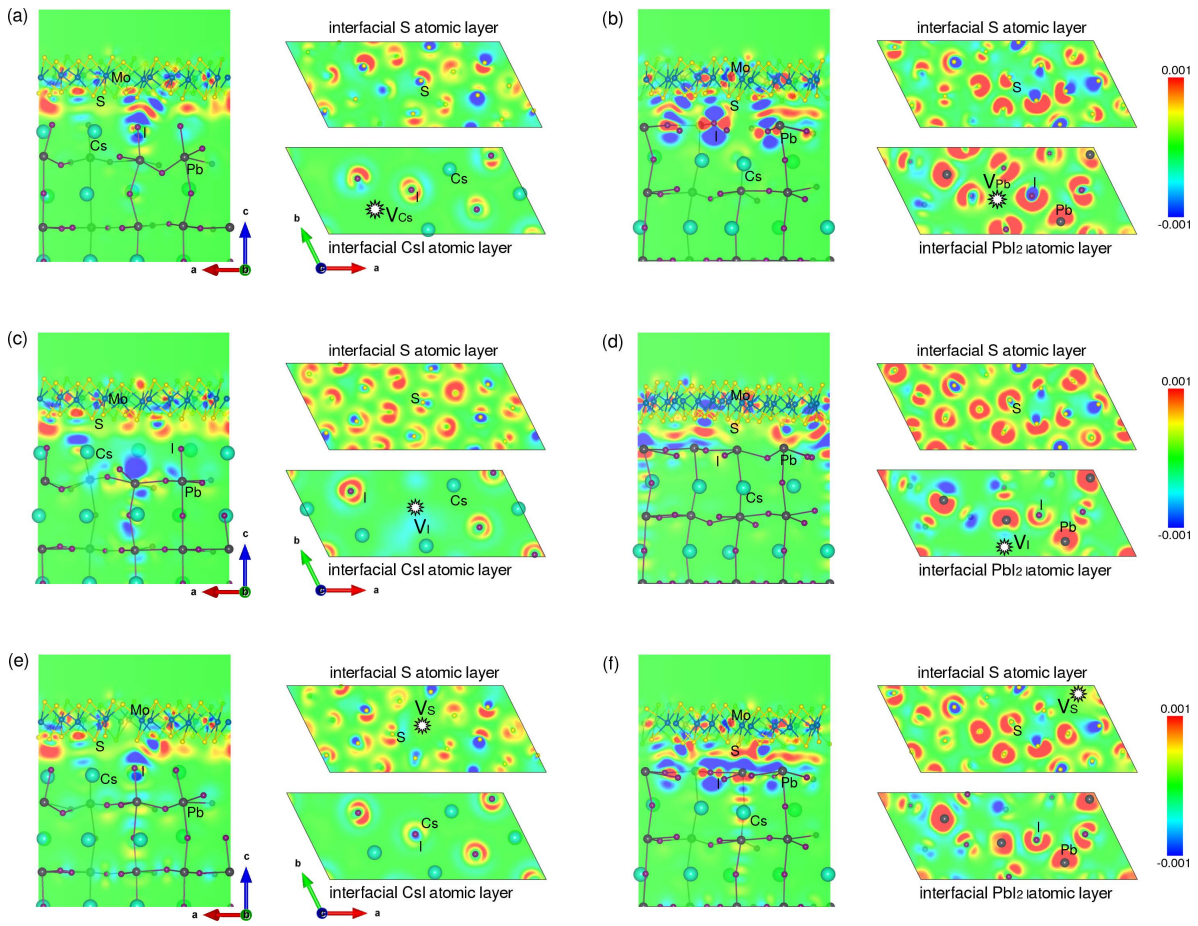

Fig. S4 Isosurface view of electron density difference at the value of 0.001 $|e|/Å^3$ upon formation of CsI/MoS_2 and PbI_2/MoS_2 interfaces. Red (blue) colour represents the electron accumulation (depletion).

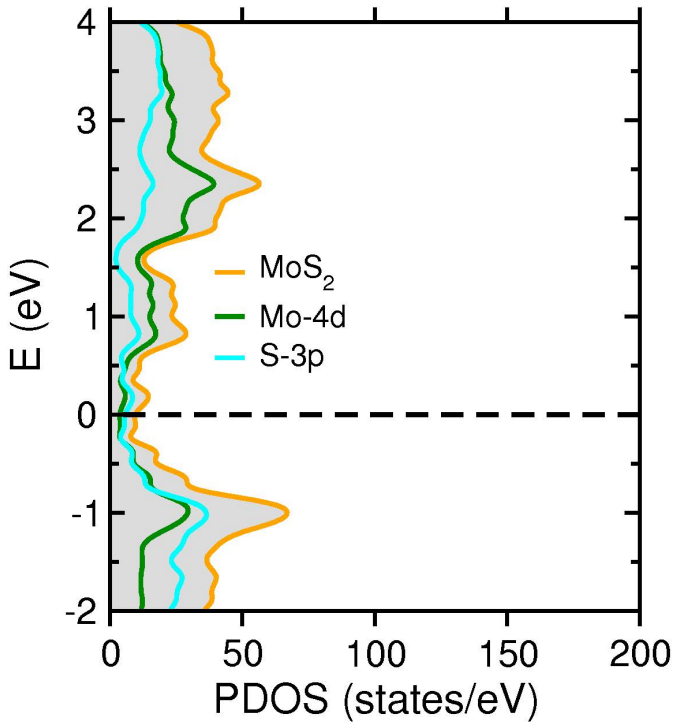

Fig. S5 PDOS of pristine 1T-MoS_2 monolayer. Dash line indicates Fermi energy level.

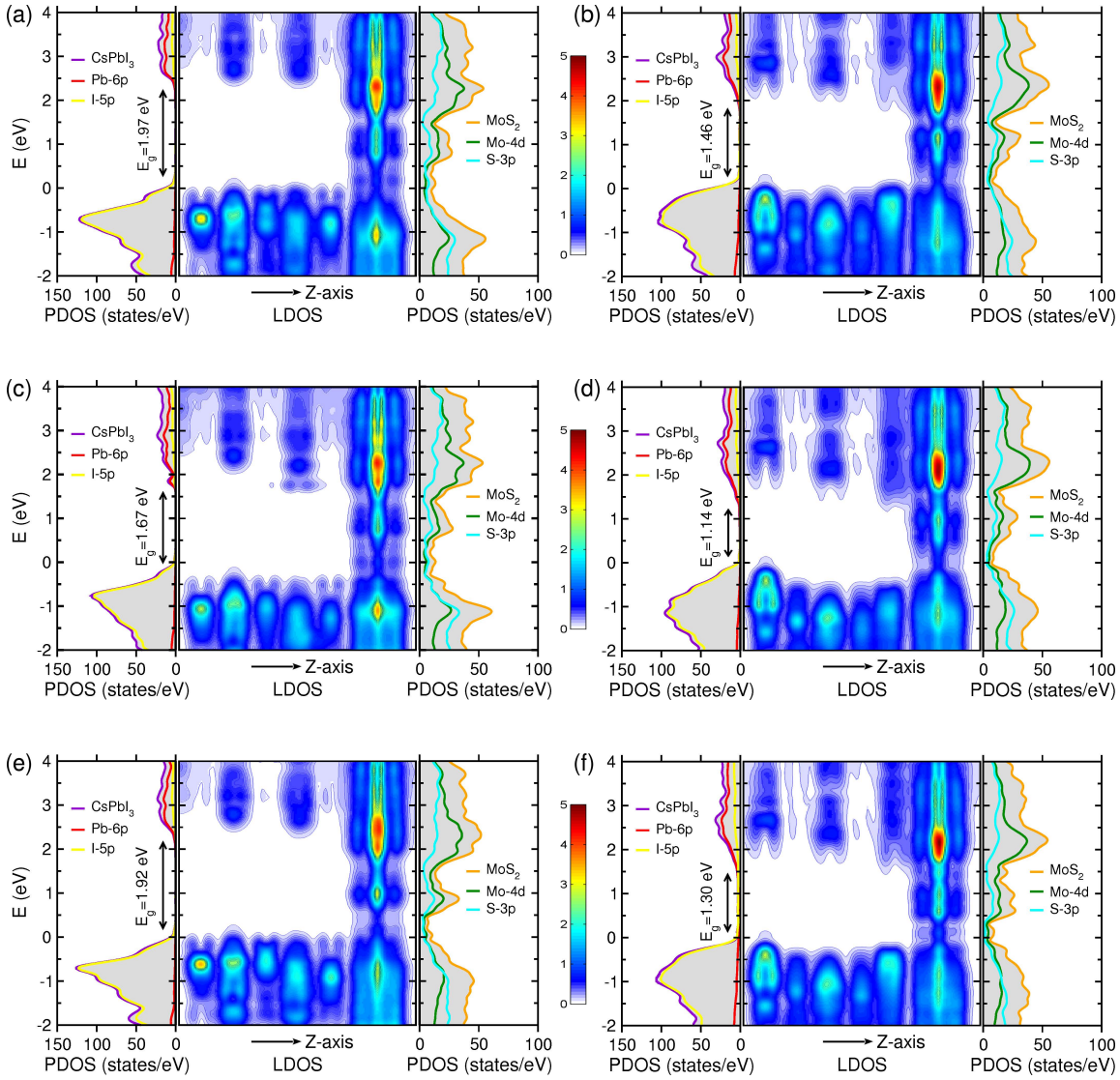

Fig. S6 PDOS from $CsPbI_3$ (left panel) and MoS_2 (right panel) parts and isoline plot of LDOS for defective CsI/MoS_2 (left column) and PbI_2/MoS_2 interfaces (right column) with a vacancy like (a) V_{Cs}, (b) V_{Pb}, (c, d) V_I and (e, f) V_S.

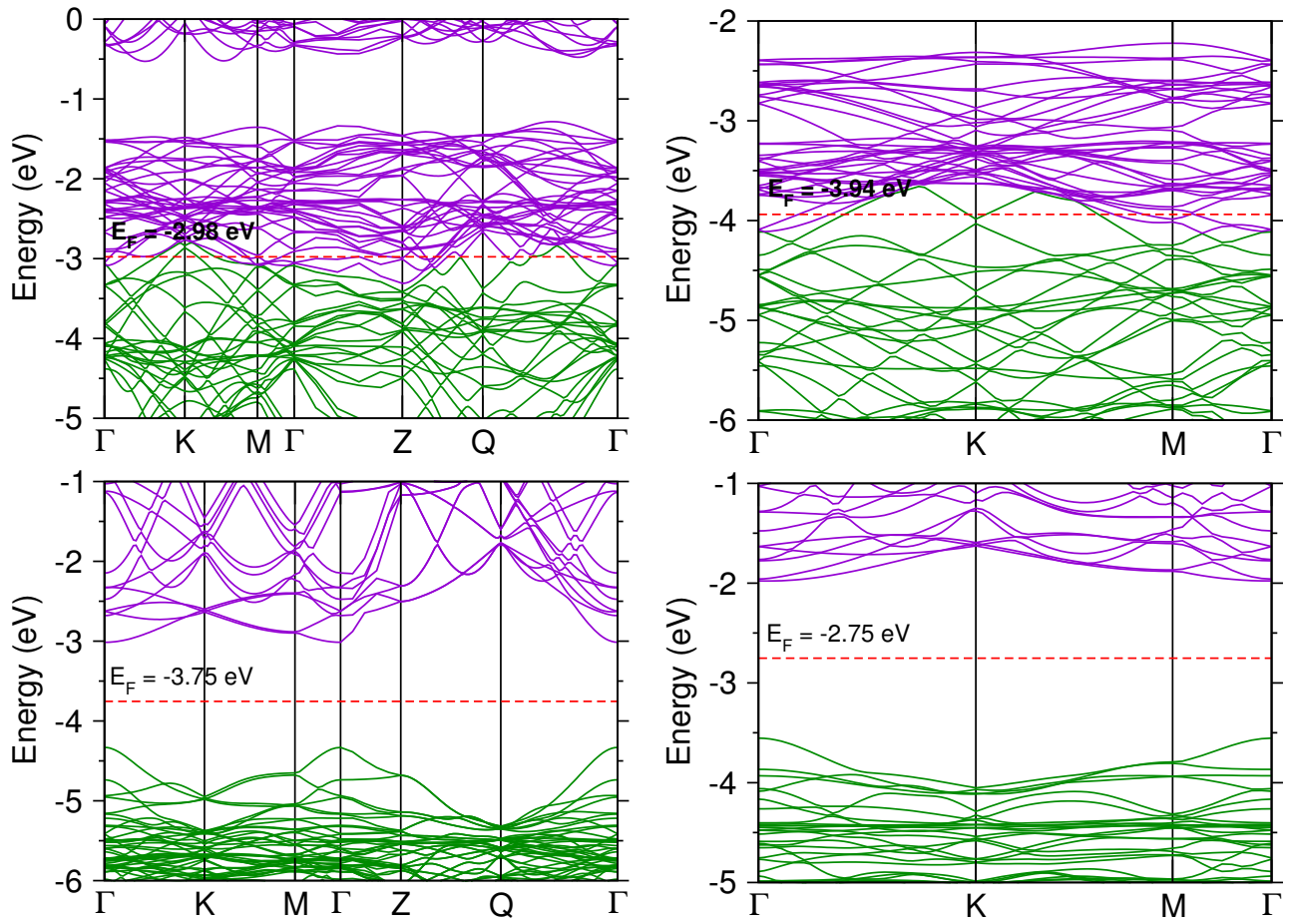

Fig. S7 Electronic band structures of 1T-MoS_2 (top panel) and β-$CsPbI_3$ in bulk (left panel) and surface (right panel) phases. Green and violet colours represent the occupied and empty bands, respectively. The Fermi level E_F is denoted by red-coloured dotted line.

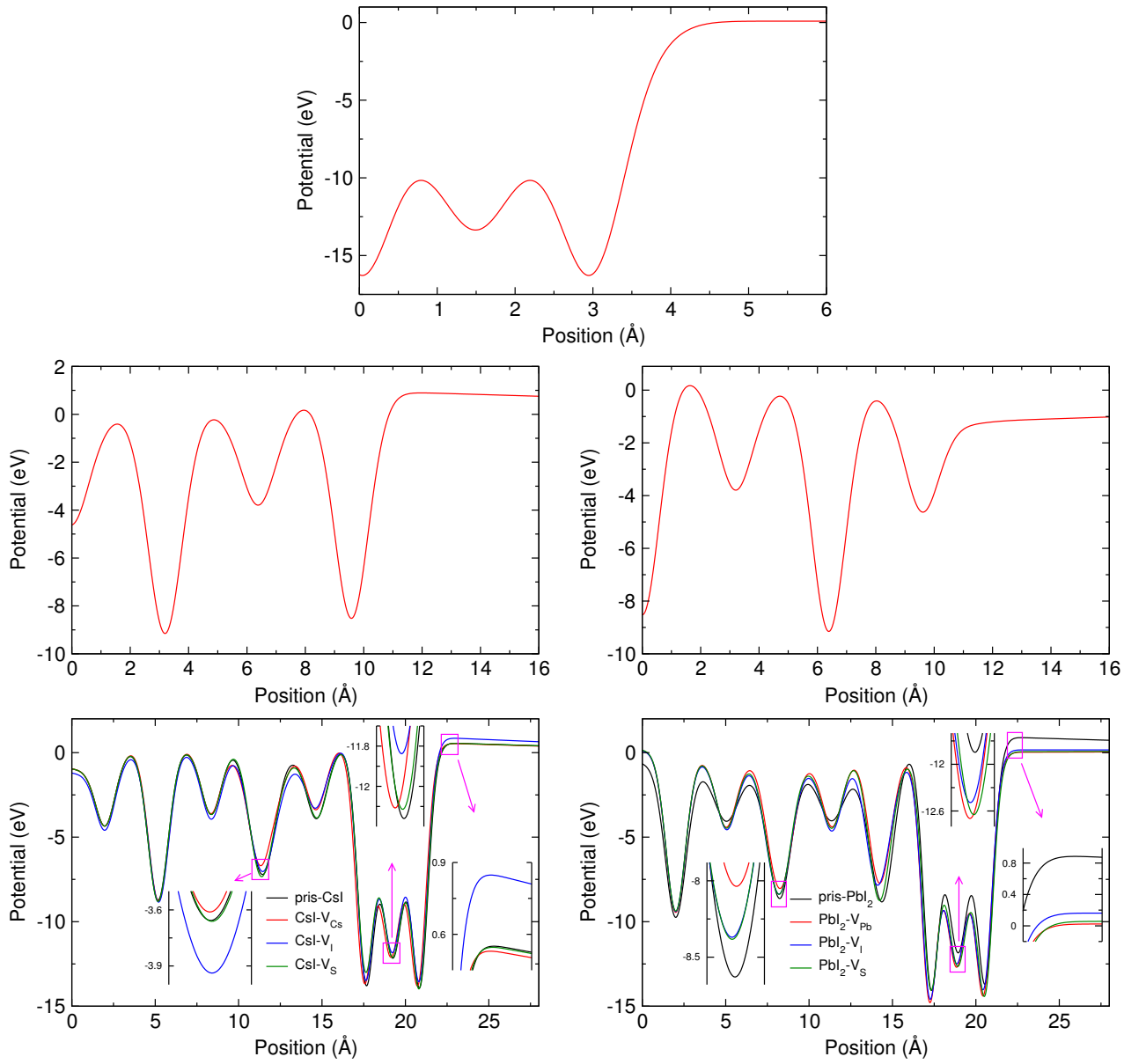

Fig. S8 Electrostatic potential in 1T-MoS_2 surface (top panel), β-$CsPbI_3$ surface (middle panel) with CsI (left) and PbI_2 (right) terminations, and interface systems (bottom panel) of CsI/MoS_2 (left) and PbI_2/MoS_2 with interfacial vacancy defects.

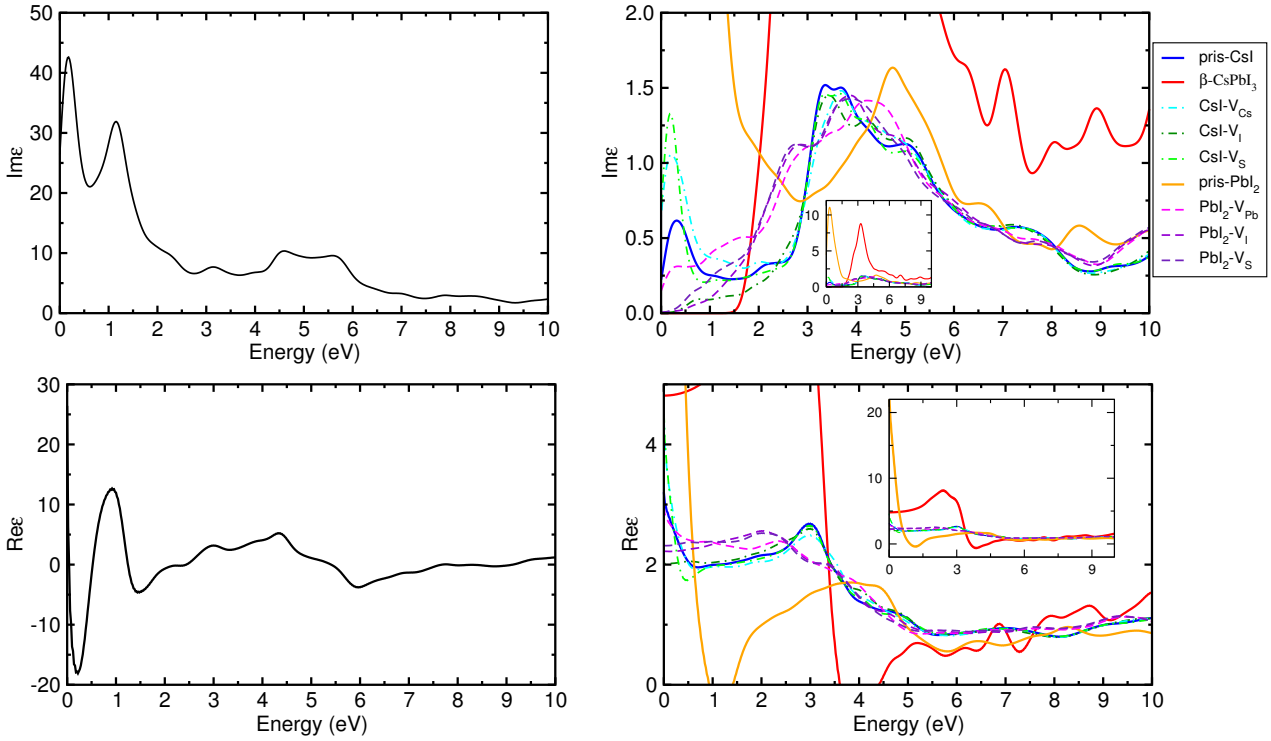

Fig. S9 Imaginary (top panel) and real (bottom panel) parts of the frequency-dependent dielectric functions for 1T-MoS_2 bulk (left panel) and other systems (right panel), such as β-$CsPbI_3$ bulk and the interface systems.

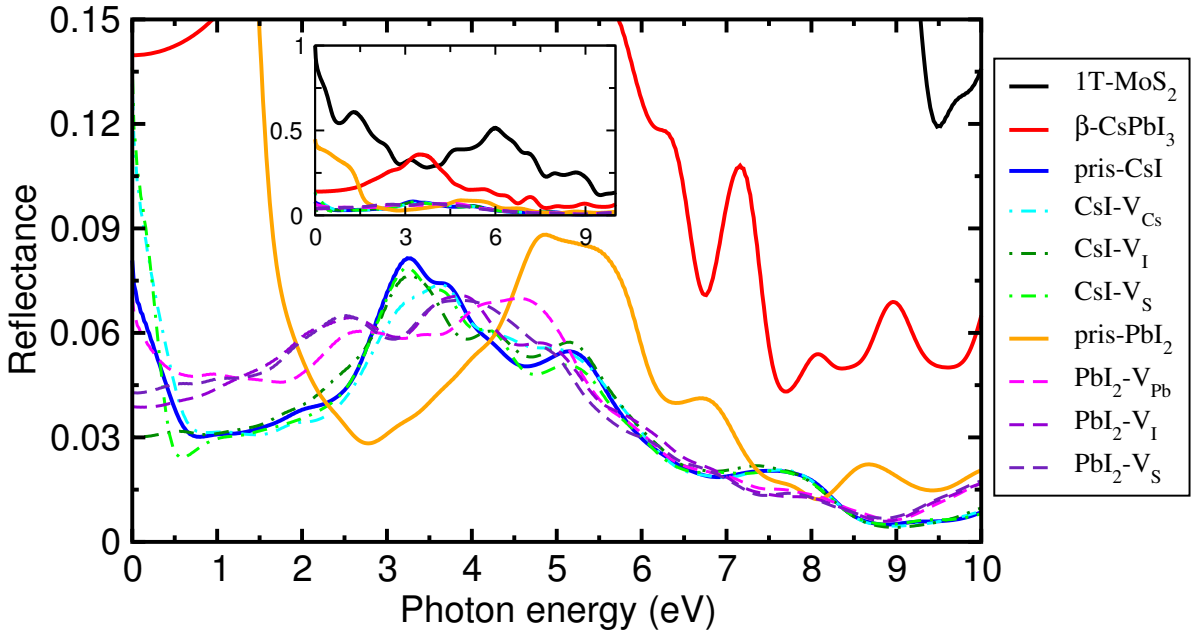

Fig. S10 Reflectance of bulks such as the 1T-MoS_2 and β-$CsPbI_3$ bulk and their interface systems.

References

[1] A. Marronnier, G. Roma, S. Boyer-Richard, L. Pedesseau, J.-M. Jancu, Y. Bonnassieux, C. Katan, C. C. Stoumpos, M. G. Kanatzidis and J. Even, Anharmonicity and disorder in the black phases of cesium lead iodide used for stable inorganic perovskite solar cells, *ACS Nano* **2018**, *12*, 3477–3486.

[2] Y. Wang, M. I. Dar, L. K. Ono, T. Zhang, M. Kan, Y. Li, L. Zhang, X. Wang, Y. Yang, X. Gao, Y. Qi, M. Grätzel and Y. Zhao, Thermodynamically stabilized β-$CsPbI_3$-based perovskite solar cells with efficiencies > 18%, *Science* **2019**, *365*, 591.

[3] T. Zhang, H. Zhu, C. Guo, S. Cao, C.-M. Lawrence, Z. Wang and X. Lu, Theoretical investigation on the hydrogen evolution reaction mechanism at MoS_2 heterostructures: The essential role of the 1T/2H phase interface, *Catal. Sci. Technol.* **2020**, *10*, 458–465.

[4] H. Eidsvåg, M. Rasukkannu, D. Velauthapillaia and P. Vajeeston, In-depth first-principles study on novel MoS_2 polymorphs, *RSC Adv.* **2021**, *11*, 3759.

[5] F. Wypych and R. Schollhorn, 1T-MoS_2, a new metallic modification of molybdenum disulfide, *J. Chem. Soc. Chem. Commun.* **1992**, *19*, 1386–1388.

[6] T. Tadano and S. Tsuneyuki, Quartic anharmonicity of rattlers and its effect on lattice thermal conductivity of clathrates from first principles, *Phys. Rev. Lett.* **2018**, *120*, 105901.